Novel Interneuronal Network in the Mouse Posterior Piriform Cortex

CHUNZHAO ZHANG,[1] GÁBOR SZABÓ,[2] FERENC ERDÉLYI,[2] JAMES D. ROSE,[1,3] AND **QIAN-QUAN SUN**[1,3]*

[1]Department of Zoology and Physiology, University of Wyoming, Laramie, Wyoming 82071
[2]Laboratory of Molecular Biology and Genetics, Institute of Experimental Medicine, H-1450 Budapest, Hungary
[3]Neuroscience Program, University of Wyoming, Laramie, Wyoming 82071

ABSTRACT

The neural circuits of the piriform cortex mediate field potential oscillations and complex functions related to integrating odor cues with behavior, affective states, and multisensory processing. Previous anatomical studies have established major neural pathways linking the piriform cortex to other cortical and subcortical regions and major glutamatergic and GABAergic neuronal subtypes within the piriform circuits. However, the quantitative properties of diverse piriform interneurons are unknown. Using quantitative neural anatomical analysis and electrophysiological recording applied to a GAD65-EGFP transgenic mouse expressing GFP (green fluorescent protein) under the control of the GAD65 promoter, here we report a novel inhibitory network that is composed of neurons positive for GAD65-EGFP in the posterior piriform cortex (PPC). These interneurons had stereotyped dendritic and axonal properties that were distinct from basket cells or interneurons expressing various calcium-binding proteins (parvalbumin, calbindin, and calretinin) within the PPC. The GAD65-GFP neurons are GABAergic and outnumbered any other interneurons (expressing parvalbumin, calbindin, and calretinin) we studied. The firing pattern of these interneurons was highly homogenous and is similar to the regular-spiking nonpyramidal (RSNP) interneurons reported in primary sensory and other neocortical regions. Robust dye coupling among these interneurons and expression of connexin 36 suggested that they form electrically coupled networks. The predominant targets of descending axons of these interneurons were the dendrites of Layer III principal cells. Additionally, synapses were found on dendrites and somata of deep Layer II principal neurons and Layer III basket cells. A similar interneuronal subtype was also found in GAD65-EGFP-negative mouse. The extensive dendritic bifurcation at superficial lamina IA among horizontal afferent fibers and unique axonal targeting pattern suggests that these interneurons may play a role in direct feedforward inhibitory and disinhibitory olfactory processing. We conclude that the GAD65-GFP neurons may play distinct roles in regulating information flow and olfactory-related oscillation within the PPC in vivo. J. Comp. Neurol. 499:1000–1015, 2006. © 2006 Wiley-Liss, Inc.

Indexing terms: olfaction; interneuron; GAD65,; calcium binding proteins; connexin; green-fluorescent protein (GFP); GABA; inhibitory network

The olfactory system of mammals generates field potential oscillations in the presence of odorants (Freeman, 1978). Both gamma (30–100 Hz) and theta (3–12 Hz) frequency oscillations occur in the olfactory bulb (Eeckman and Freeman, 1990; Kay and Freeman, 1998) as well as the piriform cortex (Kay et al., 1996). Studies have also shown that oscillations in these two structures are correlated (Eeckman and Freeman, 1990; Kay and Freeman, 1998). Excitatory synaptic pathways linking these two structures occur through mitral cell axons from the olfactory bulb projecting to piriform cortex (cf. Haberly and Price, 1977; Luskin and Price, 1983; Zou et al., 2001). However, the mechanisms and functional significance of

the oscillations in the piriform cortex remain to be understood. In vitro models of rhythms of cognitive relevance,

such as gamma (30–80 Hz) and theta (5–12 Hz) rhythms demonstrate an absolute requirement for phasic inhibitory synaptic transmission (Whittington and Traub, 2003; Buzsaki and Draguhn, 2004). Distinct interneuronal subtypes with different firing patterns and axonal targets (dendritic vs. somatic) may play distinct roles in the formation of different forms of oscillations (Prince, 1999; Whittington and Traub, 2003; Buzsaki and Draguhn, 2004). Eventual understanding of mechanisms underlying odorant induced oscillations in the cortex will require a thorough knowledge of interneuronal subtypes in the olfactory-piriform cortical networks.

In addition to olfactory inputs from the olfactory bulb, principal neurons in the piriform cortex also receive input from the anterior olfactory cortex and from extensive autoassociative networks in many neocortical and subcortical areas (Luskin and Price, 1983; Price, 1999, Price, 2003). This complex integrative neural circuitry may mediate functions related to integrating odor cues with behavior, assessing the emotional or motivational significance of sensory cues, multisensory association, and memory (Luskin and Price, 1983; Price, 1999, Price, 2003). In order for precise processing of olfactory and multisensory information to take place without runaway recurrent excitation in the neuronal population, excitation and inhibition must be delicately balanced (Chagnac-Amitai, 1989; Prince, 1999). Knowledge of the fine structural organization of inhibitory and excitatory microcircuits is a prerequisite for thorough understanding of the central mechanisms of olfactory processing.

GABAergic inhibitory cells contribute to oscillatory activities and sensory gating within the corticolimbic system by supplying both inhibitory and disinhibitory potentials to local circuits (Prince, 1999; Benes and Berretta, 2001). GABAergic interneurons in the cortex are assumed to provide stability to the pyramidal neurons by feedforward and feedback inhibition. It is now recognized that these interneurons form a rich variety of cortical synaptic connections (e.g., somato–dendritic, axo–somatic, dendro–dendritic) with layer-specific axonal projections and recurrent interconnections with other GABAergic cells. In addition, GABAergic interneurons are responsible for triggering and maintaining network oscillations over a wide range of frequencies (reviewed by Prince, 1999; Buzsaki and Draguhn, 2004). Such inhibitory networks can maintain population synchrony through $GABA_A$ receptors (Whittington and Traub, 2003). Therefore, as well as providing the temporal structure for excitatory networks, the GABAergic cells regulate synchronized oscillations across

forebrain, thereby enabling anatomically separated populations of neurons to interact. A number of studies have characterized the inhibitory neurons in the piriform cortex, particularly basket cells. (Haberly and Feig, 1983; Haberly, 1983; Westenbroek et al., 1987; Kubota and Jones, 1993; Ekstrand et al., 2001a,Ekstrand et al., 2001b). Using antisera to calcium binding proteins, Kubota and Jones (1993) discovered that calbindin (CB) and parvalbumin (PV) neurons in Layer III gave rise to basket endings in Layer II. A more quantitative analysis by Ekstrand et al. (Ekstrand et al. 2001a,Ekstrand et al. 2001b) revealed a highly diverse population of basket cells that express a large number of combinations of molecular markers (GAD65, GAD67, VIP, CCK, PV, and CB), morphological characteristics (bitufted, pyramidal-like, multipolar, etc.), and laminar distributions of dendrites and axons. In contrast, studies dealing with dendritic targeting and nonbasket cells are absent. In addition, quantitative analysis of morphological and electrophysiological properties of a diverse group of interneurons in the piriform cortex is lacking. In the neocortex, particularly sensory neocortices (including somatosensory, visual, and auditory; reviewed by Markram et al., 2004) and hippocampus (McBain and Fisahn, 2001), such detailed analysis has provided important insight into the functional properties of diverse inhibitory networks. Taking advantage of a transgenic mouse, in which subgroups of GABAergic neurons express bright green fluorescent protein (GPF) under the promoter of GAD65 (Lopez-Bendito et al., 2004), here we report a novel inhibitory network that is composed of interneurons that are positive for GAD65-EGFP. These neurons had unique laminar localization (predominantly Layer IIa), stereotypical dendritic arborization and axonal targeting pattern, and were the most abundant GABAergic cell types in both the anterior and posterior piriform cortex. Due to differences in cytoarchitecture between anterior and posterior division and complexity in the subdivisional composition in the anterior piriform cortex (Ekstrand et al., 2001b), detailed quantitative analysis of the morphological properties of these neurons were focused on the posterior division. Within PPC, these interneurons showed a unique firing pattern (regular-spiking nonpyramidal type, RSNP) that has not been reported in the interneurons of the piriform cortices. Additionally, there was little overlap between GAD65-EGFP cells and interneurons expressing various calcium-binding proteins, parvalbumin, calretinin, and calbindin. We hypothesize a role of the GAD65-GFP neurons in direct olfactory mediated feedforward inhibitory and disinhibitory processing.

MATERIALS AND METHODS

All experiments were carried out using a protocol approved by the University of Wyoming Institutional Animal Care and Use Committee.

GAD65-GFP transgenic mouse line

This mouse was originally developed at the Department of Gene Technology and Developmental Neurobiology, Institute of Experimental Medicine in Budapest, Hungary. Generation and analysis of transgenic mice expressing GFP under the control of the GAD65 promoter has been described in detail elsewhere (Lopez-Bendito et al., 2004). For this study, heterozygous transgenic mice on C57Bl6

Abbreviations

APC	Anterior piriform cortex
CamKII	Calcium/calmodulin-dependent protein kinase II
CB	Calbindin
CR	Calretinin
GAD	Glutamate decarboxylase
IR	Immunoreactivity
GABA	γ-Aminobutyric acid
GFP	Green fluorescent protein
LOT	Lateral olfactory tract
NF-M	Intermediate neurofilament
Pir	Piriform cortex
PPC	Posterior piriform cortex
PV	Parvalbumin
RSNP	Regular-spiking nonpyramidal

The Journal of Comparative Neurology. DOI 10.1002/cne

1002   **C. ZHANG ET AL.**

background were used from line GAD65_3e/gfp5.5 30. In the studied line, a 6.5-kb segment of the GAD65 gene that includes 5.5 kb of the 5′ upstream region, the first two exons, and a portion of the third exon with the corresponding introns drives the expression of GFP almost exclusively to the GABAergic neurons in many brain regions including the neocortex (Lopez-Bendito et al., 2004).

Brain slice preparations and intracellular dye injection

To test dye coupling among GFP cells, live brain slices were made based on methods described previously (Sun et al., 2003a,Sun et al., 2003b). Briefly, GAF65-GFP mice (5–8 weeks postnatal) were deeply anesthetized with pentobarbital sodium (55 mg/kg) and decapitated. The brains were quickly removed and placed into cold ($\sim$4°C) oxygenated slicing medium. The slicing medium contained (in mM): 2.5 KCl, 1.25 NaH_2PO_4, 10.0 $MgCl_2$, 0.5 $CaCl_2$, 26.0 $NaHCO_3$, 11.0 glucose, and 234.0 sucrose. Brain slices were prepared according to methods described by Agmon and Connors (1991). Tissue slices (300 μm) were cut using a vibratome (TPI, St. Louis, MO) and transferred to a holding chamber before recording. Individual slices were then transferred to a recording chamber fixed to a modified microscope stage. Slices were minimally submerged and continuously superfused with oxygenated physiological saline at a rate of 4.0 mL/min. The physiological perfusion solution contained (in mM): 126.0 NaCl, 2.5 KCl, 1.25 NaH_2PO_4, 1.0 $MgCl_2$, 2.0 $CaCl_2$, 26.0 $NaHCO_3$, and 10.0 glucose. Solutions were gassed with 95% O_2 / 5% CO_2 to a final pH of 7.4 at a temperature of 35 ± 1°C. A potassium based patch pipette solution containing 5% neurobiotin (Vector Laboratories, Burlingame, CA) was used for making patch clamp recordings from GFP-expressing neurons. Standard patch recordings were performed for at least 1 hour before slices were fixed in 4% paraformaldehyde. GFP neurons were initially identified under an epifluorescent microscope. We then switched to infrared DIC microscopy for visualized patch-clamp recording (e.g., Figs. 3, 9).

Fixation and immunohistochemistry

Brains were postfixed after perfusion in 4% paraformaldehyde at 4°C overnight, cryoprotected in 30% sucrose for 2 days, frozen, and cut into 30-μm thick cryostat sections. Free-floating sections were then stained for antibody-DAB as follows: sections were rinsed in phosphate-buffered saline (PBS, pH 7.4), incubated for 30 minutes in 0.5% H_2O_2 in PBS, 2 × 10-minute PBS washes, incubated for 2 hours at room temperature in PBS with 0.3% Triton X-100, 0.05% Tween, and 4% normal goat serum, and incubated overnight at 4°C in PBS containing 0.2% Triton X-100 and primary antibodies directed against: PV (1:1,000, Calbiochem, La Jolla, CA) or GFP (1:1,000, polyclonal chicken anti-GFP, Chemicon, Temecula, CA). Sections were then rinsed two times in PBS, incubated at room temperature for 90 minutes in PBS containing biotinylated goat anti-rabbit IgG (Vector Labs) for PV or biotinylated goat anti-chicken IgG (Vector Labs) for GFP, and finally incubated overnight at 4°C in Vectastain ABC kit (Vector Labs). Sections were then rinsed two times in PBS, developed in 50 mM TBS (pH 7.4) containing 0.04% 3,3′-diaminobenzidine tetrahydrochloride (DAB, Sigma-Aldrich, St. Louis, MO) and 0.012% H_2O_2, washed two times with TBS, mounted onto glass slides, dehydrated,

cleared, and coverslipped. 3D neuron models were reconstructed from stained cells using the Neurolucida system (MicroBrightField, Williston, VT) and a brightfield light microscope (Carl Zeiss MicroImaging, Thornwood, NY). Shrinkage was not corrected. Reconstructed neurons were quantitatively analyzed with NeuroExplorer (MicroBrightField).

Double and triple immunohistochemical labeling

Brains were postfixed after perfusion in 4% paraformaldehyde at 4°C overnight, cryoprotected in 30% sucrose for 2 days, frozen, and cut into 30-μm thick cryostat sections. Free-floating sections were then stained for antibodies as follows: sections were rinsed in PBS, incubated for 30 minutes in 0.5% H_2O_2 in PBS, washed 2 × 10 minutes in PBS, incubated for 2 hours at room temperature in PBS with 0.3% Triton X-100, 0.05% Tween, and 4% normal goat serum, and incubated overnight at 4°C in PBS containing 0.2% Triton X-100 and primary antibodies directed against PV (1:1,000, Calbiochem). The other primary antibodies used were: a polyclonal rabbit anticonnexin 36 (1:125, Zymed Laboratories, Invitrogen, South San Francisco, CA), a polyclonal rabbit anticalretinin antibody (1:500, Sigma), a polyclonal rabbit anticalbindin antibody (1:1000, Sigma), a polyclonal rabbit anticalmodulin-dependent protein kinase II (1:1,000, Chemicon), a polyclonal rabbit anti-GAD65&67 (1:1,000, Chemicon), a polyclonal rabbit antineurofilament (1:500, Chemicon), a polyclonal chicken anti-GFP (1:1,000, Chemicon), and a monoclonal mouse anti-NeuN (neuronal nuclei antigen, mAb A60, Chemicon). Sections were then rinsed two times in PBS and incubated for 3 hours at room temperature in Alexa Fluor 594, goat antirabbit IgG (heavy and light chains) for PV. The sections were then rinsed, mounted, and coverslipped using Vectashield mounting medium with or without DAPI. The immunofluorescent specimens were examined using an epifluorescence microscope (Carl Zeiss) equipped with AxioCam digital color camera. Double or triple immunofluorescent images were analyzed using an AxioVision LE imaging suite (Carl Zeiss). Confoal microscopy images were sampled using an upright Nikon E800 microscope and Bio-Rad (Hercules, CA) Radiance 2100 image analysis software suits. Photomicrographs were processed using Photoshop CS2 (Adobe Systems, San Jose, CA). Necessary modifications (such as adjusting contrast and intensities) were performed to improve the quality of the original photomicrographs.

RESULTS

Distribution of the GAD65-EGFP interneurons

In this study the lamination of the piriform cortex was determined by immunostaining of specific neuronal marker NeuN (Figs. 1B, 2C) (cf. Mullen et al., 1992). The laminar location of the GAD65-EGFP interneurons was based on terminology described earlier by Haberly and Price (1978). Abundant GAD65-GFP neurons were found in Layer II of both the anterior and posterior divisions of the PPC (Figs. 1, 2). The density of GFP neurons was slightly but significantly higher in the posterior than the anterior divisions (0.0020 ± 0.0005 vs. 0.0013 ± 0.0003

The Journal of Comparative Neurology. DOI 10.1002/cne

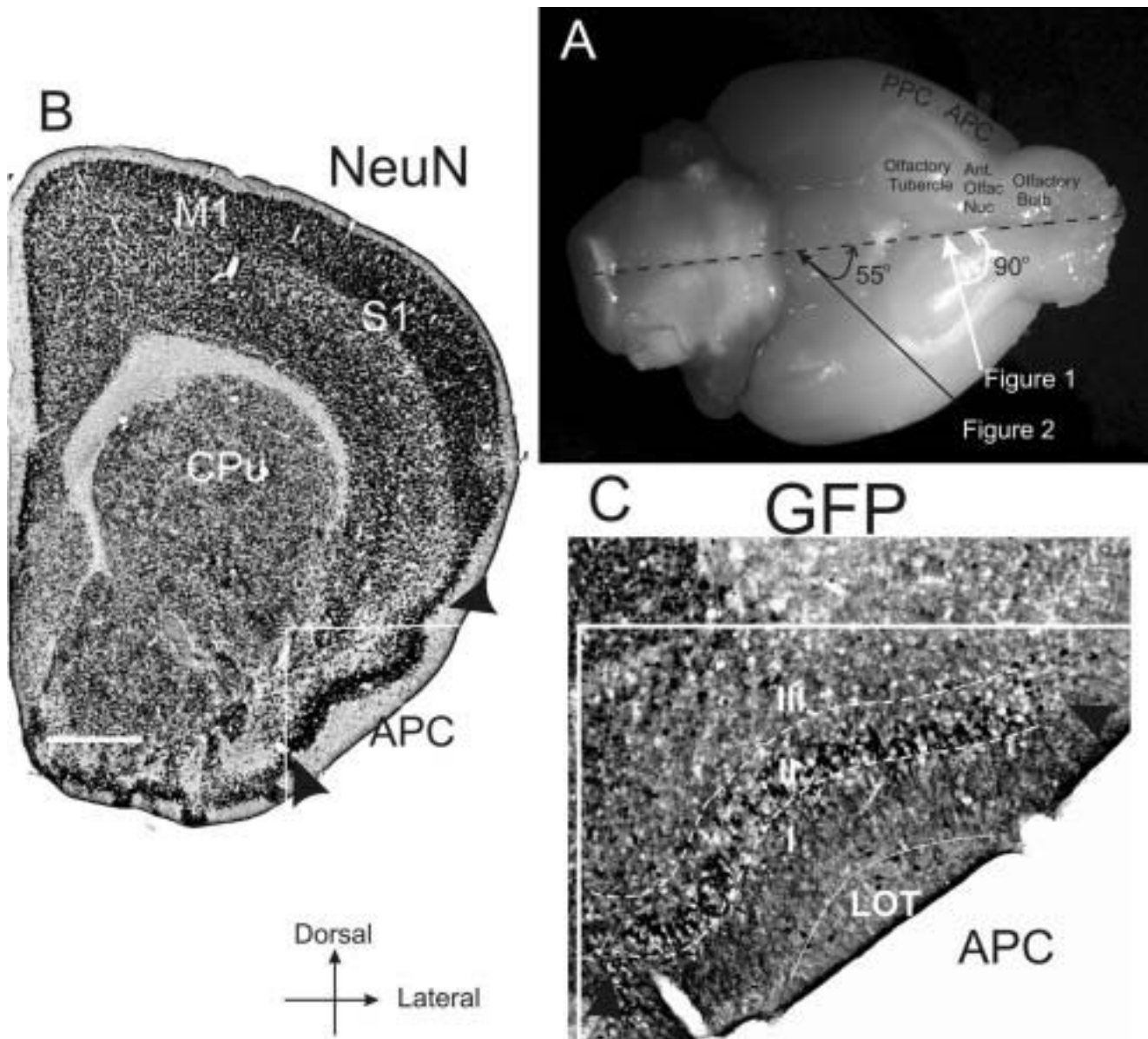NOVEL OLFACTORY INHIBITORY NETWORKS 1003

Fig. 1. **A:** Ventral aspect of mouse brain, slightly tilted for optimal view of olfactory cortex. White arrow shows coronal section level for Figure 1 (APC), black arrow shows tilted (thalamocortical) section level for Figures 2–10 (PPC). **B:** A coronal section through anterior piriform cortex (0.5 mm Bregma), stained with antibodies to NeuN. The NeuN staining shows how Pir consists of a cell-dense Lamina II and cell-sparse Lamina III. Arrowheads mark dorsal and ventral boundaries of piriform cortex (Pir) as defined in Materials and Methods. **C:** An adjacent section (from B, area demarcated by solid white lines) stained with antibodies to GFP. Abundant EGFP-positive cells are found in Lamina II. Scale bar = 250 μm in B.

cells μm^2; $P < 0.01$; n = 8 sections from 4 brains). The somatodendritic morphology of these GFP neurons appears similar. Due to differences in cytoarchitecture between the anterior and posterior division, and complexity in the subdivisional composition in the anterior piriform cortex (Ekstrand et al., 2001b), detailed quantitative analysis of the morphological properties of these neurons were focused on the posterior division. The distribution of the GAD65-EGFP neurons in the posterior piriform cortex was unique among all cortical regions (Fig. 2). The location of the GAD65-EGFP neurons within the piriform cortex was layer-specific, i.e., most of the GAD65-EGFP neurons were located throughout Layer II (Fig. 3). This layer-specific pattern was consistent throughout the entire posterior piriform cortex (Fig. 2A). On average, the distance of GAD65-EGFP neuronal somata to the pia surface was 267 ± 6 μm (n = 205). These neurons were densely packed in Layer II, with an average intersoma distance of 20 ± 3 μm and an average nearest-neighbor distance of 6 ± 1 μm (n = 205). Within Layer II of the PPC, these cells constitute one-third of all the neurons (as marked by NeuN, n = 8 sections from 4 brains). This

The Journal of Comparative Neurology. DOI 10.1002/cne

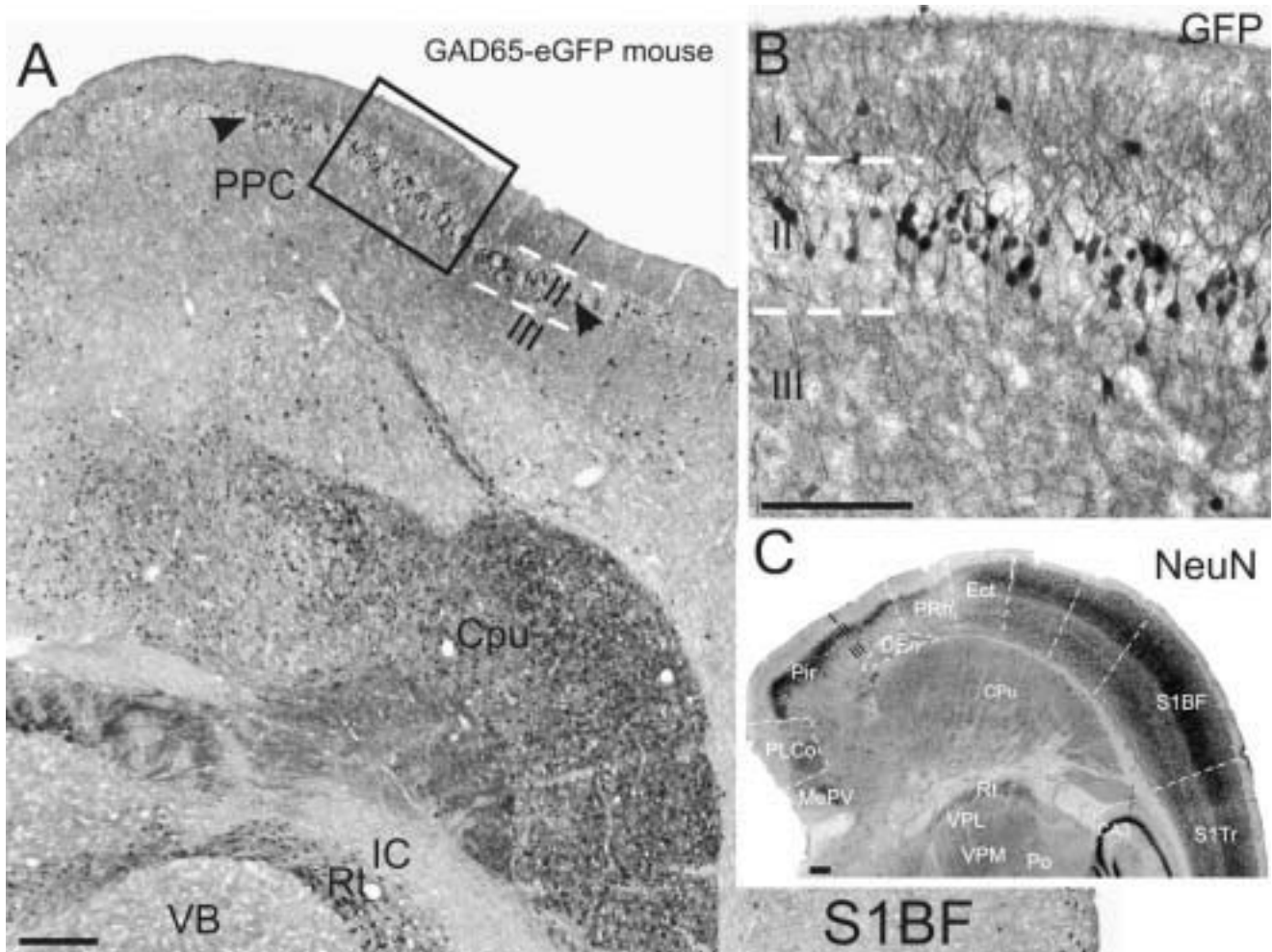1004   C. ZHANG ET AL.

Fig. 2. **A:** Thalamocortical (TC) section through posterior piriform cortex stained with antibodies to EGFP. The TC sectioning method was adopted because it preserves layer-specific cytoarchitectonic organization throughout the entire PPC (cf. Fig. 1A). Arrowheads mark dorsal and ventral boundaries of piriform cortex (Pir) as defined in Materials and Methods. Abundant EGFP-positive cells are found in the upper proportion of Lamina II. **B:** GAD65-EGFP immunohistochemistry staining of mid-Pir (box in A) shows distinct immunoarchitecture characterized by stereotyped dendritic appearance of the GAD65-EGFP cells. **C:** An adjacent section stained with antibodies to NeuN. The NeuN staining shows how Pir consists of a cell-dense Lamina II and cell sparse Lamina III. Scale bars = 250 μm.

concentration is ∼10 times higher than the density of PV cells (0.00017 ± 0.00004 cells μm²). A very small proportion of GAD65-GFP neurons were also found in upper Layer III and Layer I (Figs. 2, 3). In comparison to the piriform cortex, the laminar localization of the GAD65-EGFP neurons in neocortical regions and subcortical regions was different (Fig. 2). In the barrel cortex, sparsely scattered GAD65-EGFP neurons were found predominantly at superficial Layer II/III. In the striatum, amygdala, and nucleus reticularis, the GAD65-EGFP cells were scattered (Fig. 2). Quantitative analysis of the GAD65-GFP neurons in the neocortical region was published in an earlier study (Lopez-Bendito et al., 2004).

Soma-dendritic and axonal morphology of GAD65-EGFP neurons

The somata of these neurons were relatively small (perimeter 55 ± 2 μm, n = 100), with an ovoid shape and a form factor value of 0.6 ± 0.02 (the value for a perfect circle is 1). The mean value for the cross-sectional cell body areas for these cells is 137 ± 9 μm². The long and short axes of the cell bodies are 12 ± 0.4 and 9.4 ± 0.5 μm, respectively (n = 8 sections from 4 brains). The dendritic arborization of the GAD65-EGFP neurons was stereotyped (Figs. 2–5). In 60% of the GAD65-EGFP cells, dendrites extended from the upper poles of the cell body to produce an ascending single tufted dendritic tree (e.g., Figs. 3, 4). In 20% of the cells, both ascending and descending dendrites formed bitufted dendritic trees.

In a majority of these cells the ascending tuft of dendrites was frequently much more profuse than the descending tuft, with the diameter of the upward dendrites usually gradually tapered toward the end. Most of the primary dendrites branched close to the cell body, while additional branching sometimes occurred more distally (Figs. 2–4). The branches of the ascending dendrites were
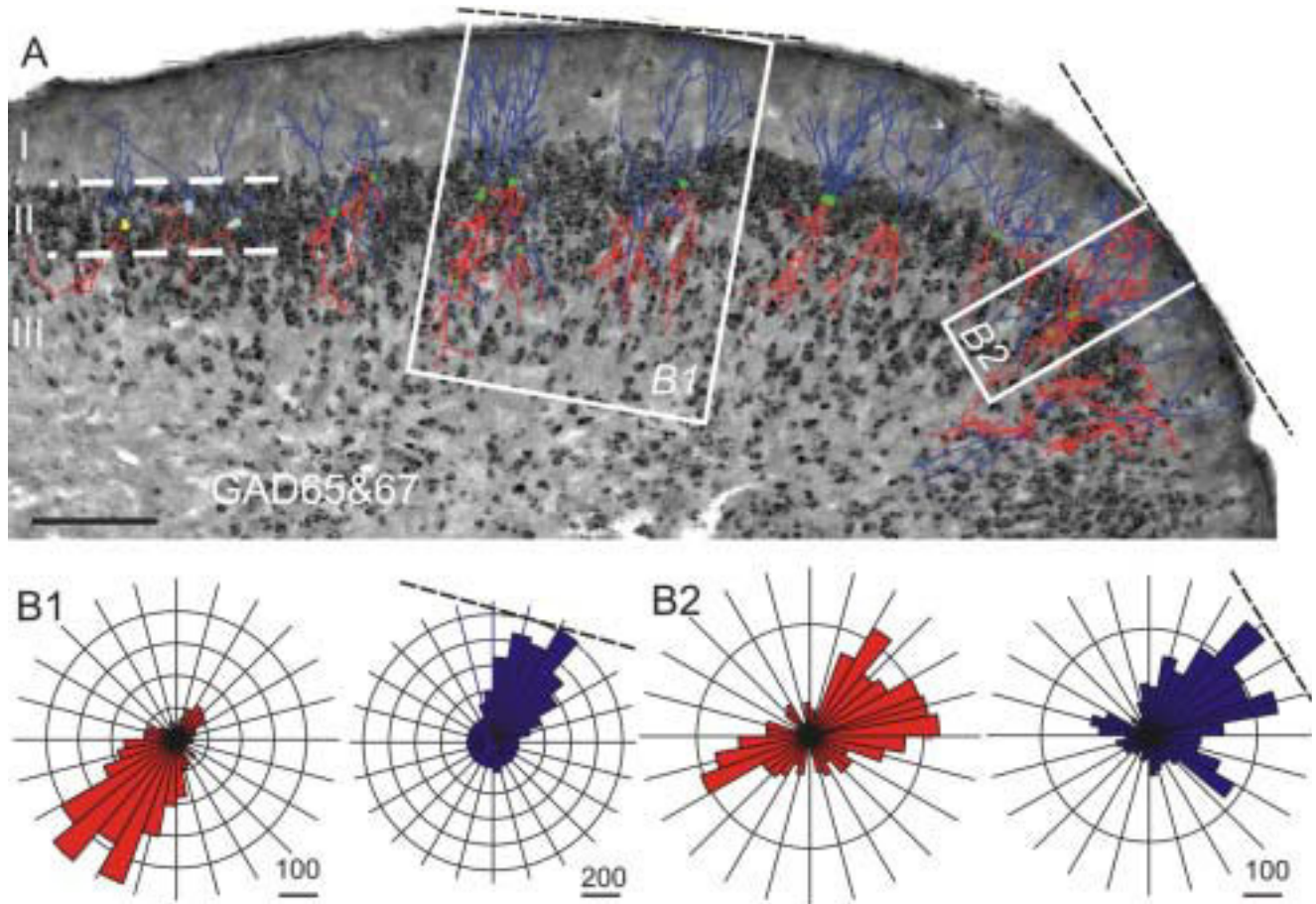
The Journal of Comparative Neurology. DOI 10.1002/cne

NOVEL OLFACTORY INHIBITORY NETWORKS

1005

Fig. 3. **A:** Camera-lucida montage of GAD65-EGFP cells in the Pir Laminae II/III from a single 40-μM section, superimposed on an adjacent section stained with antibodies to GAD65&67. Blue: dendrites; red: axons. Most cells in Lamina II show bitufted dendrites and descending axons that enter Layer III. Cells in deeper Layer II or Layer III have multipolar dendrites and axons projecting locally or extending to Layer II. **B:** Morphological analysis of the polar histogram (length as function of direction) of dendrites (blue) and axons (red) of the cells located in the yellow (B1) or green (B2) box of A (n = 10 cells). Note that both the dendrites and the axons had a narrower distribution in the mid Pir. Dashed lines in A-C are tangential to the pia surface. Scale bar = 250 μm in A; 100 or 200 μm in B (as shown).

typically oriented in narrow clusters toward the pia surface. These dendrites often reached the outer portion of Layer I (pia surface) and overlapped with horizontally oriented axons in this layer (e.g., Fig. 5A2). Both the basal and distal dendrites had a cylindrical shape and were largely aspiny or sparsely spiny.

The axons of the GAD65-EGFP cells emerged directly from the cell body. The initial portion of the axonal trunk, which was usually thick (diameter 0.5 ± 0.05 μm), typically descended, giving off collateral branches. These collaterals projected at opposite angles from the main dendritic tree (Figs. 3, 4) and branched on average 7 ± 0.6 times to give rise to a profuse plexus in the vicinity of the parent cell body. The axonal plexus of a single cell occupied an area of 495 ± 87 μm^2 (n = 30). The depth it occupied varied and appeared to be contained within a cylindrical space of 60 ± 6 μm^3. The majority of the segments of the axons were located 250–350 μM away from the pia surface and this number sharply declined in regions deeper than 400 μm. Therefore, these neurons predominantly targeted neurons in deep Layer II (IIb) cells and cells in upper Layer III.

Relationship to principal neurons

The laminar location of somata and dendrites of the GAD65-EGFP neurons was compared with known molecular markers positive for pyramidal neurons in the piriform cortex. The calcium/calmodulin-dependent protein kinase II (CaMKII) was shown to be expressed only in the glutamatergic neurons, but not in the GABAergic neurons in the piriform cortex (Zou et al., 2002) and other brain structures (McDonald et al., 2002; Benson et al., 1991, Benson et al., 1992). Double immunofluorescent labeling of CaMKII and GAD65-EGFP showed that GFP neurons and CaMKII immunoreactivities were nearly mutually exclusive (Fig. 5). A high level of CaMKII immunoreactivity was found in all three cell layers. The highest level of CaMKII expression occurred in the upper Layer II (IIa) neurons (Fig. 5B2). The cell bodies and proximal dendrites of the GAD65-EGFP cells were intermingled between the CAMKII-positive cells (Fig. 5B). The second marker we used was for intermediate neurofilaments (NF-M), which are typical structures of the neuronal cytoskeleton. In the neocortex of all species examined, these antibodies label
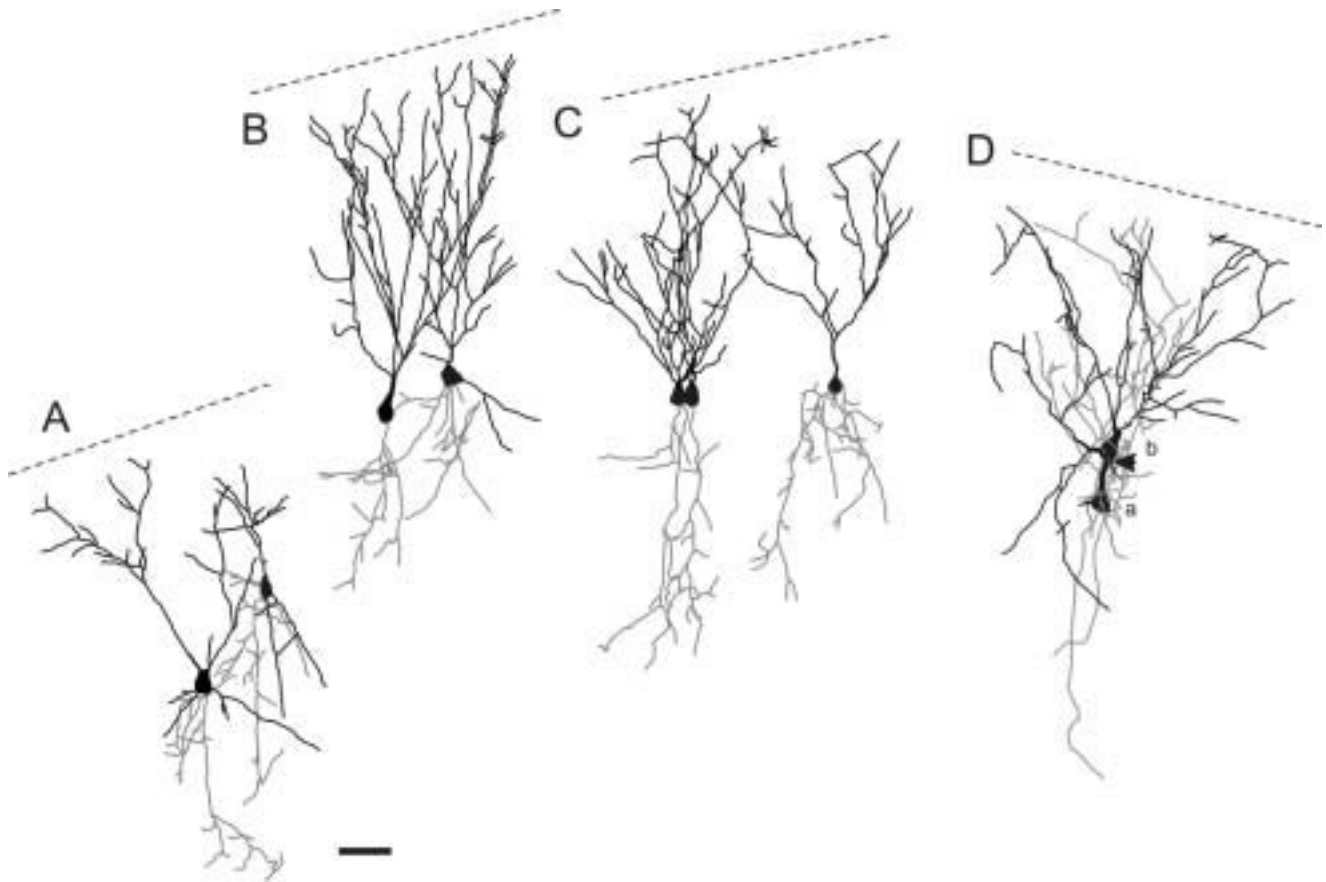
The Journal of Comparative Neurology. DOI 10.1002/cne

1006   C. ZHANG ET AL.

Fig. 4. Camera lucida montage of GAD65-EGFP cells in the PPC Laminae II/III from a single 40-μM section. Black: cell bodies and dendrites; gray: axons. Most cells in Lamina II show ascending bitufted dendrites and descending axons that enter Layer III. Cells in D and A were located on the ventral lateral and dorsal lateral boarder of PPC, respectively. Black arrowhead: main dendrite of cell "a" is in close proximity to cell "b." Scale bar = 100 μm.

pyramidal cells (Hayes and Lewis, 1992; Hornung and Riederer, 1999). In the PPC there was abundant NF-M immunoreactivity in outer Layer I (Fig. 5A2). There were also abundant vertically and horizontally oriented NF-M-positive fibers in Layers I, II, and III. The diameter and morphology of the NF-M-positive neurons in Layers II and III were reminiscent of large dendrites of pyramidal neurons (Figs. 5A2, 11A1). Double immunolabeling showed that the distal dendrites of the GAD65-EGFP neurons were highly overlapping with the NF-M-positive fibers in the upper Layer I (Fig. 5A), suggesting that the GAD65-EGFP neurons may interact with excitatory inputs arriving via Layer I. The GAD65-EGFP neurons themselves were not NF-M-positive.

To identify the location of GAD65-EGFP synapses, we performed double immunolabeling experiments. The results showed that abundant overlap of GAD65-EGFP axons and varicosities occurred on the distal and proximal dendrites of NF-M-positive neurons (Fig. 10A1), on somata and proximal dendrites of CamKII-positive neurons (Fig. 10A3), and GAD65&67-positive neurons (Fig. 10B1). The third marker we used was polyclonal rabbit anti-GAD65&67. In the piriform cortex, GAD-immunopositive perisomatic rings of boutons were found predominantly in the principal neurons (Ekstrand et al., 2001a,Ekstrand et al., 2001b). Similarly, the GAD65&67-positive cells were abundantly packed in Layer II (Figs. 5C2, 10B1). The majority of these cells were presumed pyramidal neurons, the remainder were GAD65-EGFP interneurons (asterisk in Fig. 10B1) and perhaps other types of interneurons. Inhibitory synapses of the GAD65-EGFP neurons were also abundant at the perisomatic sites on GAD65&67 positive neurons (Fig. 10B1).

GAP junction coupling

Whole-cell patch-clamp recording was performed from GAD65-EGFP-positive cells (e.g., Fig. 5). A single GFP neuron was injected with neurobiotin in each experiment. In five of six experiments we found dye-coupling among GAD65-EGFP neurons. Typically, the coupled cell bodies were in close proximity and the dendrites intermingled (Fig. 6). In particular, dendrites originating from cell *a* were often found to end in close proximity to cell *b* (e.g., Fig. 6). Using double immunolabeling of the GAD65-EGFP neurons with antibodies to the gap junction protein connexin 36 (Liu and Jones, 2003; Sohl et al., 2005), we found that connexin 36 was indeed highly expressed in these neurons (Fig. 10B3). Consistent with dye-coupling results, dendro-dendritic, dendro-somatic, and soma-
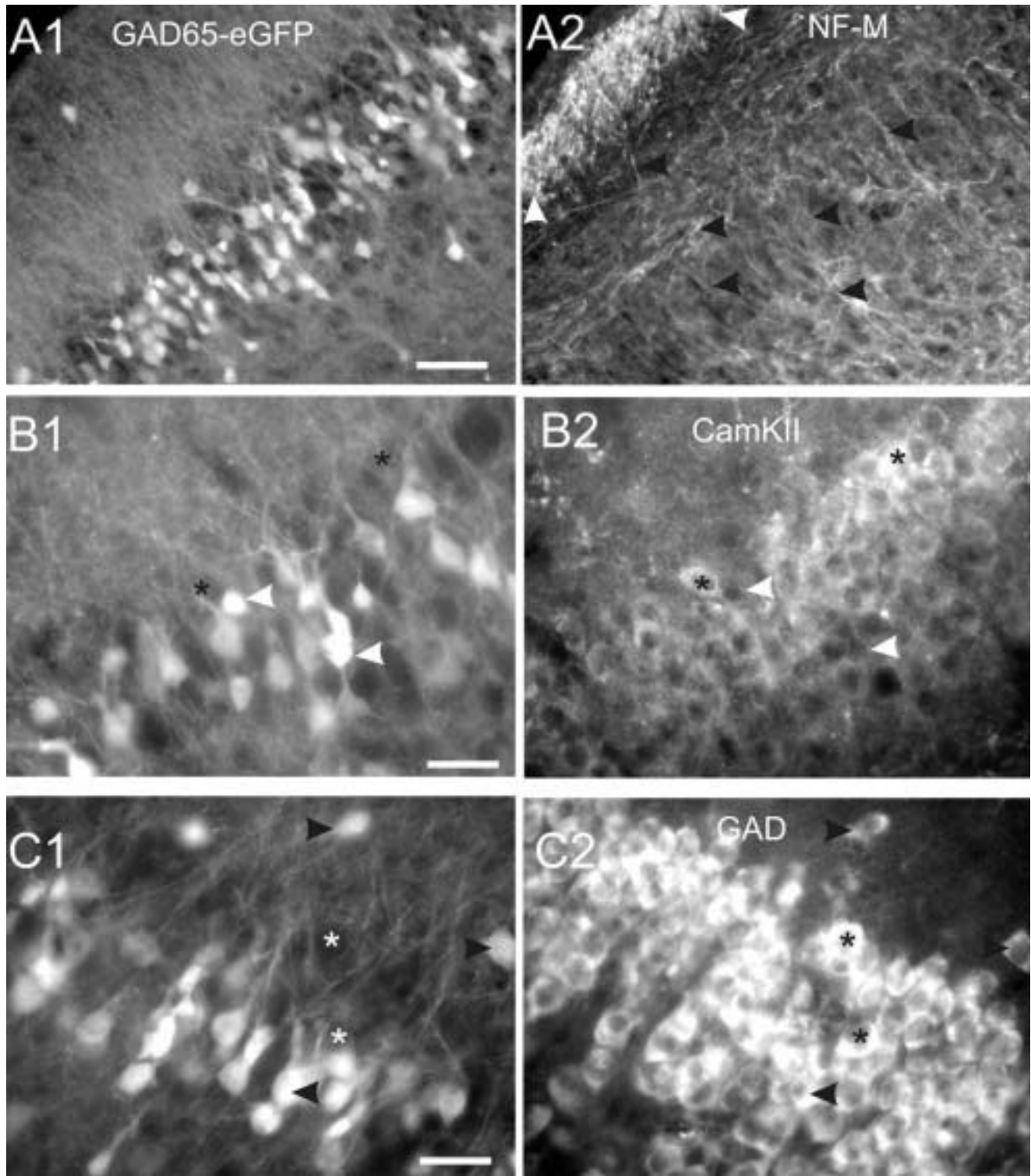
Fig. 5. Laminar location of GAD-65 GFP cells and their relation to principal neurons. **A:** Double labeling for GFP (A1), neurofilament (NF-M, A2) in mid-PPC. Large white arrowheads in A2 show a dense plexus of NF-positive fibers in Lamina IA. Smaller black arrowheads show NF-positive horizontally and vertically oriented fibers, presumed dendrites. **B**: Double labeling for GFP (B1) and Cam kinase II (CamKII, B2) in mid-PPC. The GFP-positive interneurons are mostly lacking immunoreactivity for CamKII (e.g., cell indicated with arrowhead) and vice versa (i.e., cells that are immunopositive for CamKII, cells indicated with an asterisk, are not GFP-positive). **C:** Double labeling for GFP (C1) and GAD65&67 (C2) in central PPC. Note that some GFP cells are positive for GAD (black arrowheads), but GAD-positive cells may not be GFP-positive (cells indicated with an asterisk). Scale bar = 100 μm in A; 50 μm in B,C.

The Journal of Comparative Neurology. DOI 10.1002/cne

1008   C. ZHANG ET AL.
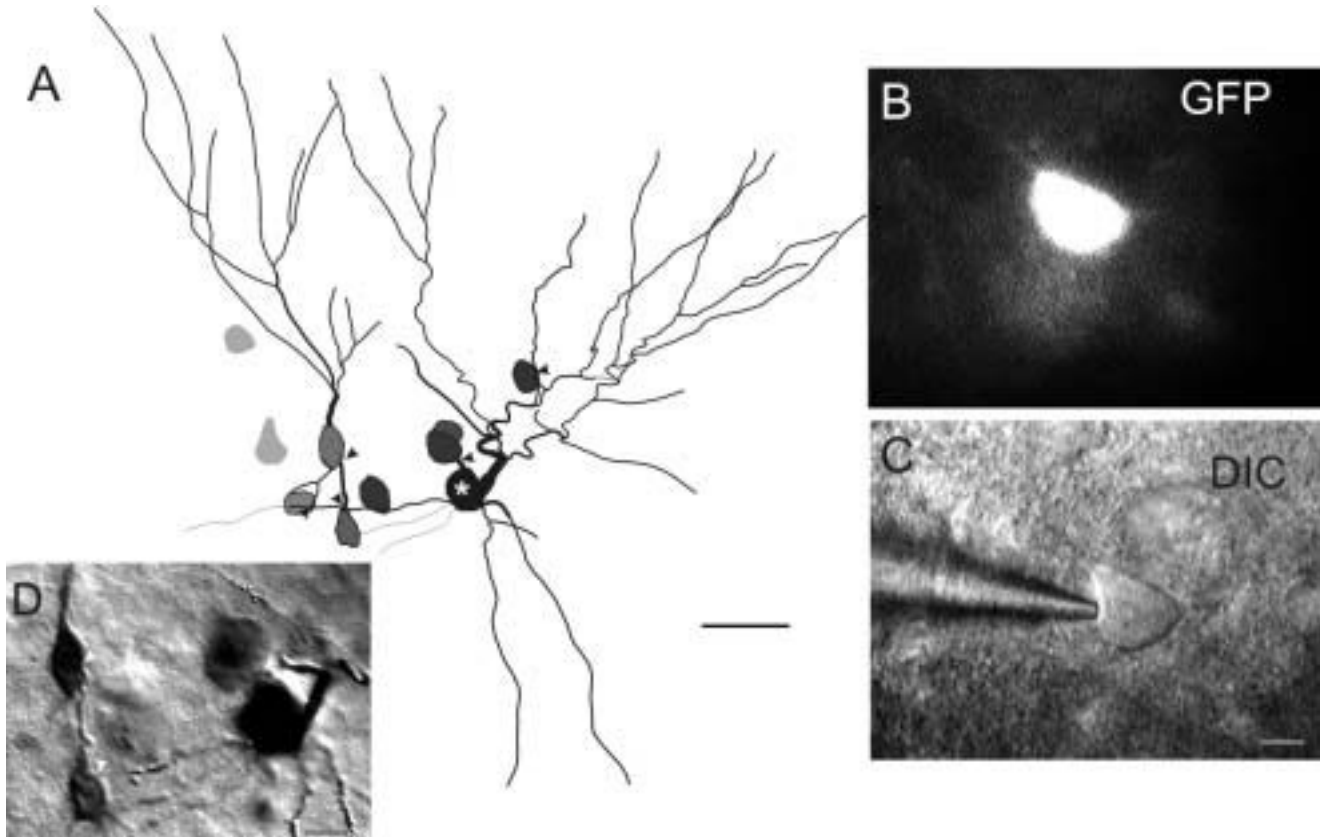
Fig. 6. **A:** Camera lucida drawing of dye-coupled GAD65-EGFP neurons labeled via intracellular recording from a GAD65-EGFP cell. Infrared D.I.C. (**C**) and epifluorescence (**B**) images of the cell prior to electrical recording. Arrows: dendrites of cell (*) were identified under a 100× oil immersion objective as appearing to form contact with another neuron. **D:** under A1: a photomicrograph of the cells in A1, showing dendrites of these cells form close contacts (white arrowheads) with cell bodies of other cells. Scale bars = 50 μm in A; 20 μm in D. Scale bars = 30 μm in A, 7.5 μm in C and D.

somatic connexin 36 immunoreactivity was found in GAD65-EGFP neurons (Fig. 10B3).

Comparison to PV-expressing neurons

Laminar distribution. In contrast to the laminar localization of the GAD65-EGFP cells, which predominantly resided in upper Layer II (Figs. 2–5), the cell bodies of the PV cells were most abundant in deep Layer II and upper Layer III (Figs. 7–9, 10C1) and their average distance to the pia surface was 367 ± 25 μm (n = 70). The cell density of PV cells was less than the GAD65-EGFP cells in Layer II. The average distance between two PV cells in all layers was 55 ± 5 μm (n = 70), which was the 2.5 times the average distance of GAD65-EGFP cells. The nearest-neighbor distance was 8 ± 2 μm (n = 70), which was 1.6 times the distance of the GAD65-EGFP cells. These results suggest that the total number of GAD65-EGFP cells in the piriform cortex far exceeded the number of PV cells.

Soma-dendritic and axonal morphology of PV inter-neurons. The somata of PV neurons were relatively small (perimeter 56 ± 3 μm, n = 70), with a multiangular shape in most cases, and a form factor value of 0.5 ± 0.1. PV cells displayed a variety of dendritic morphologies, most being basically multipolar, with longer vertical than horizontal dendrites (Figs. 8, 9). The dendrites possessed a moderate density of spines (not shown). The axons usually descended or ascended before giving off horizontal collaterals. Many of the PV immunopositive axons showed a vertical orientation similar to their dendritic arbors (Fig. 9). However, there were many PV cells that had axons originating from any orientation and following a variety of trajectories (e.g., Fig. 8B2,B3). The axons of PV cells formed a dense plexus in Layer II (Fig. 8), which spread across the whole PPC region. In Layer II the axons followed a tortuous path between cell bodies, forming abundant perisomatic buttons around unlabeled cells (Fig. 8B1). The axonal plexus from each cell occupied an area of 294 ± 56 μm² (n = 40). The distribution of these axon segments had two distinct zones. The first and larger zone of the axonal segments was located at ~250 μm (Layer II) away from the pia surface and the second and smaller peak was located ~475 μm (Layer III, not shown). Therefore, the PV neurons target neurons predominantly located in Layer II, and to a less extent neurons in Layer III.

Coexpression of calcium-binding proteins and relationship to other interneurons

Calretinin (CR). Calretinin neurons were sparsely scattered in Layers I, II, and III of the PPC. The dendrites of the CR-expressing neurons showed bipolar,

The Journal of Comparative Neurology. DOI 10.1002/cne
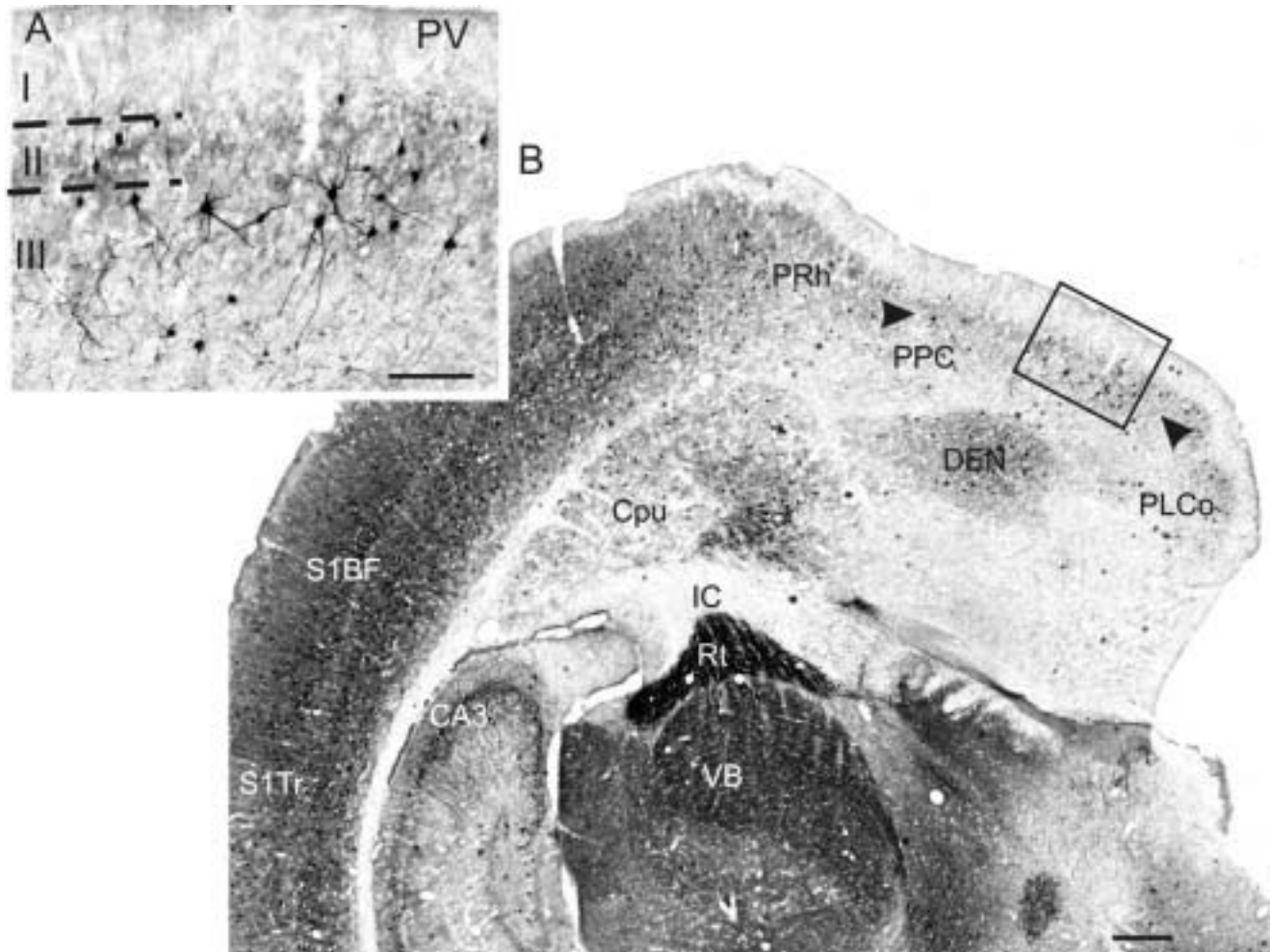
NOVEL OLFACTORY INHIBITORY NETWORKS

1009

Fig. 7. **A:** Parvalbumin (PV)-immunopositive cells (from box in the whole section in B) whose dendrites show multipolar formation. **B:** Thalamocortical (TC) section through posterior piriform cortex stained with antibodies to PV. Arrowheads mark dorsal and ventral boundaries of the posterior piriform cortex (PPC) defined in Materials and Methods. PV-positive cells can be found through Laminae II and III. Scale bars = 250 μm in A; 400 μm in B.

bitufted, tripolar, or single tufted formation (Fig. 9A). A small proportion of GAD65-EGFP neurons (<2%, n = 25 slices; e.g., Fig. 9A) coexpressed CR. For CR neurons, 15% (n = 100) were also GFP-positive (e.g., Fig. 3A2).

Calbindin (CB). CB-positive neurons were spread through PPC Layers I, II, and III. Their dendrites were short, with tripolar or multipolar formations. A small proportion of GAD65-EGFP neurons (<2%, n = 25 slices; e.g., Fig. 9B) coexpressed CB.

Parvalbumin. There was virtually no overlap between PV-expressing neurons and GAD65-EGFP neurons (Fig. 9C).

GABA. In all, 80% of GAD65-EGFP neurons (n = 205) were also positive for GABA, although the levels of expression differed between neurons (e.g., Fig. 10B2). GAD65-EGFP-positive puncta, presumed synaptic terminals, were also positive for GABA. A small proportion (15%) of GABA-positive cells (n = 200) in Layer II of PPC did not express EGFP.

Firing properties of the GAD65-GFP neurons

We made whole-cell patch-clamp recordings from GAD65-GFP neurons located in the PPC. A brief depolarization (8 ms, 60 pA) of the membrane induced a single action potential in these neurons with a half width of 1.3 ± 0.3 ms (n = 8 cells, Table 1). Firing patterns of the GAD65-GFP cells were all very similar. The details of these properties are shown in Table 1. Application of prolonged depolarization (>100 ms) induced repetitive spike trains that showed very weak spike adaptations. The interspike frequency at near threshold stimulation was 9 ± 1 Hz (n = 8) and increased linearly with increased depolarization current. Maximum interspike frequency was 65 ± 4Hz (n = 8). There were no apparent fast or slow after hyperpolarization (AHPs) recorded in these cells. These neurons had a near rest membrane resistance of 165 ± 25 M° (n = 8). In addition, burst or rebound burst discharges were never observed, even when the mem-
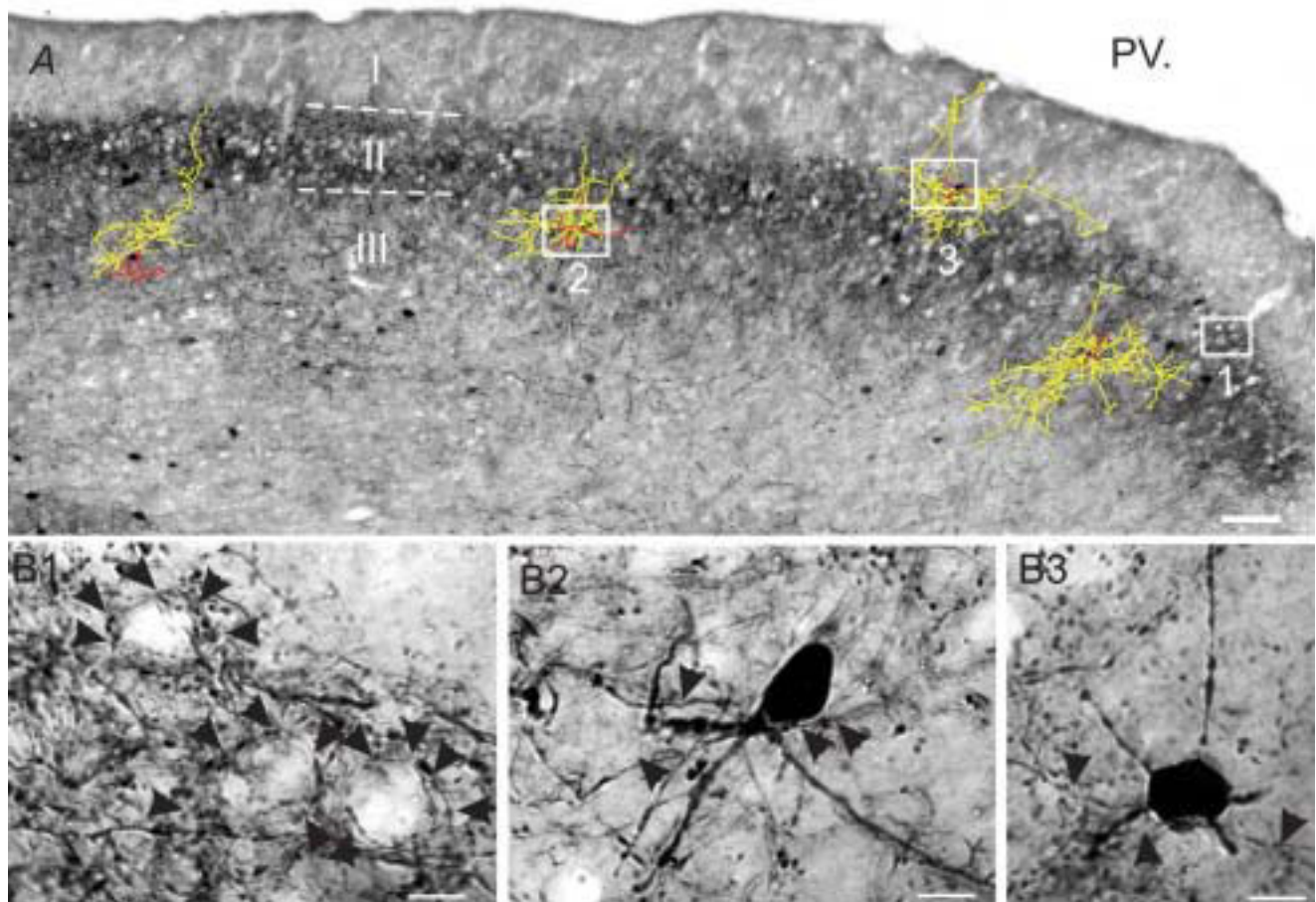
Fig. 8.   **A:** Camera lucida montage of parvalbumin (PV). Cells in the posterior piriform cortex (PPC) Laminae II and III from a single 40-μM stained section, superimposed on the same section stained with antibodies to PV. Note that the PV immunoarchitecture is characterized by very dense terminal labeling in Lamina II. Red: dendrites, yellow: axons. **B1:** Rings of darkly stained boutons (arrowhead) outline unstained cell bodies in Layer II. This picture is enlarged from box 1 in A. **B2,3:** Two cells positive for PV. Arrowheads: axon branches derived from axonal initial portion. Cells in B2 and B3 are the cells shown in boxes 2 and 3 in A. Scale bars = 100 μm in A; 10 μm in B.

brane potentials of these neurons were held at more negative values (-70 mV, not shown). These properties were similar to RSNP in the somatosensory cortex (Beierlein et al., 2003; Sun et al., 2006).

Verification of the interneuronal subtype in the GFP-negative mouse

Finally, to test whether interneurons with similar laminar location, dendritic morphology, and axon pattern also existed in GFP-negative mouse species, we performed whole-cell patch-clamp recordings in GFP-negative littermates. Cells were loaded with neurobiotin while recordings were made. We found that, indeed, interneurons with similar dendritic and axonal arborization patterns and laminae location also existed in these non-GFP mice (e.g., Fig. 11A vs. B). The properties of a single action potential, such as half-width (1.2 ± 0.4 ms, n = 6), input resistance (138 ± 33, n = 6), near threshold interspike frequency (11 ± 2 Hz, n = 6), maximum interspike frequency (69 ± 6Hz, n = 6), and resting membrane potential (-66 ± 4 mV, n = 6) were similar to the GAD65-GFP cells (Table 1). The pattern of repetitive spike trains was also similar to

the GAD65-GFP cells (data not shown). These data indicate that interneurons with morphological and physiological properties similar to the GAD65-GFP cells also existed in the PPC of wildtype mice.

DISCUSSION

The neural circuits of the piriform cortex are thought to mediate complex functions related to integrating odor cues with behavior, affective states, and multisensory processing (Luskin and Price, 1983; Price, 1999, Price, 2003). However, knowledge of the fine structural organization of inhibitory microcircuits is incomplete. A detailed understanding of these microcircuits will be fundamental to a detailed explanation of piriform cortex function. Previous results showed that the densities of GABAergic neurons in the posterior piriform cortex were much higher than in the anterior piriform cortex (Haberly, 1983; Loscher et al., 1998). However, the composition of interneuronal subtypes in the posterior piriform cortex has not been examined in detail. For example, it was unclear whether there is any layer-specific distribution of a particular interneu-
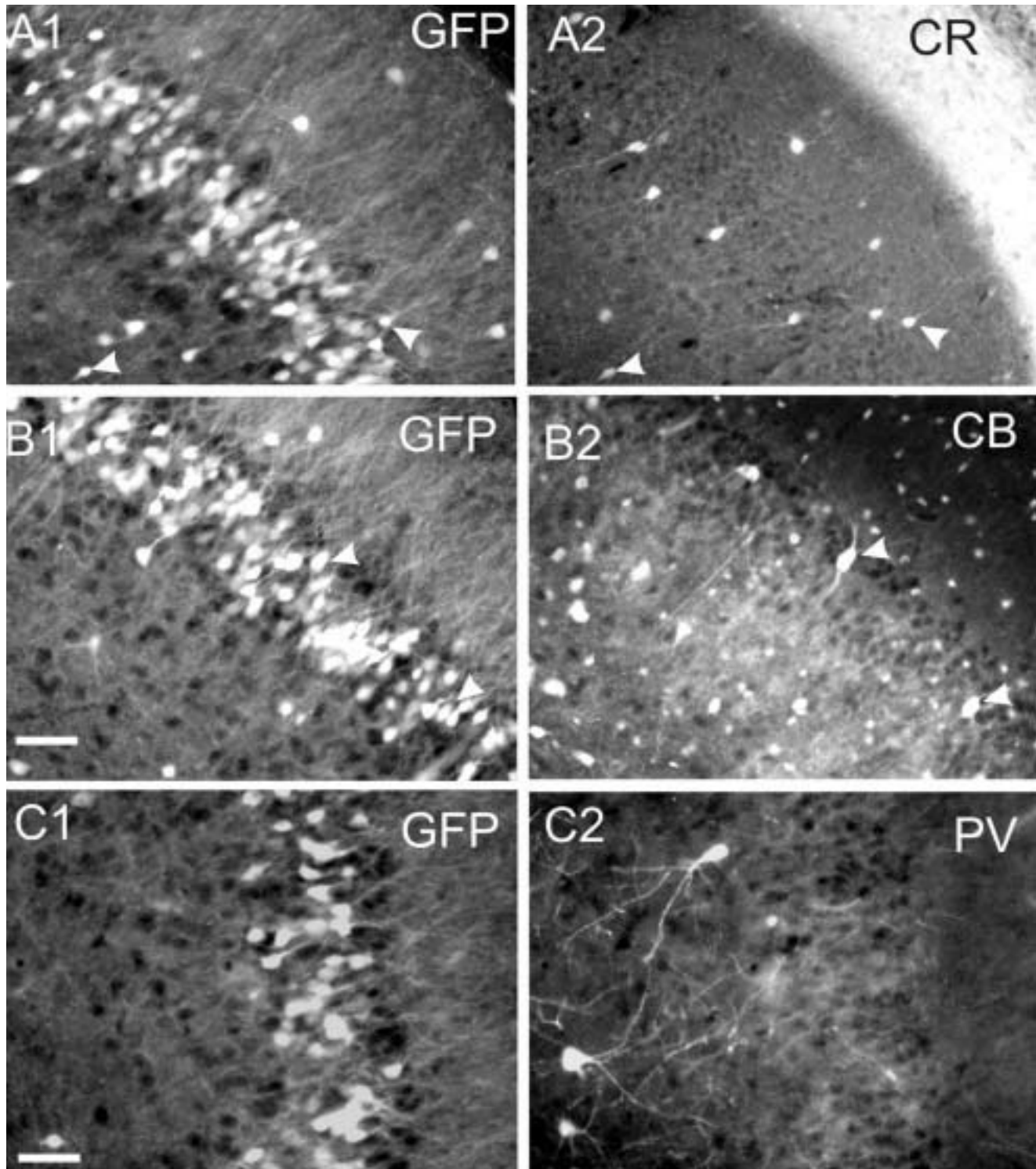
Fig. 9. **A:** Double labeling for GFP (A1) and CR (A2) in mid-PPC. The GFP-positive interneurons are mostly lacking immunoreactivity for CR, except for two neurons marked with white arrowheads, which show neurons positive for both CR and GFP. **B:** Double labeling for GFP (B1), CB (B2) in mid-PPC. The GFP-positive interneurons are mostly lacking the immunoreactivity for CB, except for two neurons marked with white arrowheads, which are positive for both CB and GFP. **C:** Double labeling for GFP (C1) and PV (C2) in central PPC. Note that none of the GFP cells expressed PV. Scale bars = 50 μm.
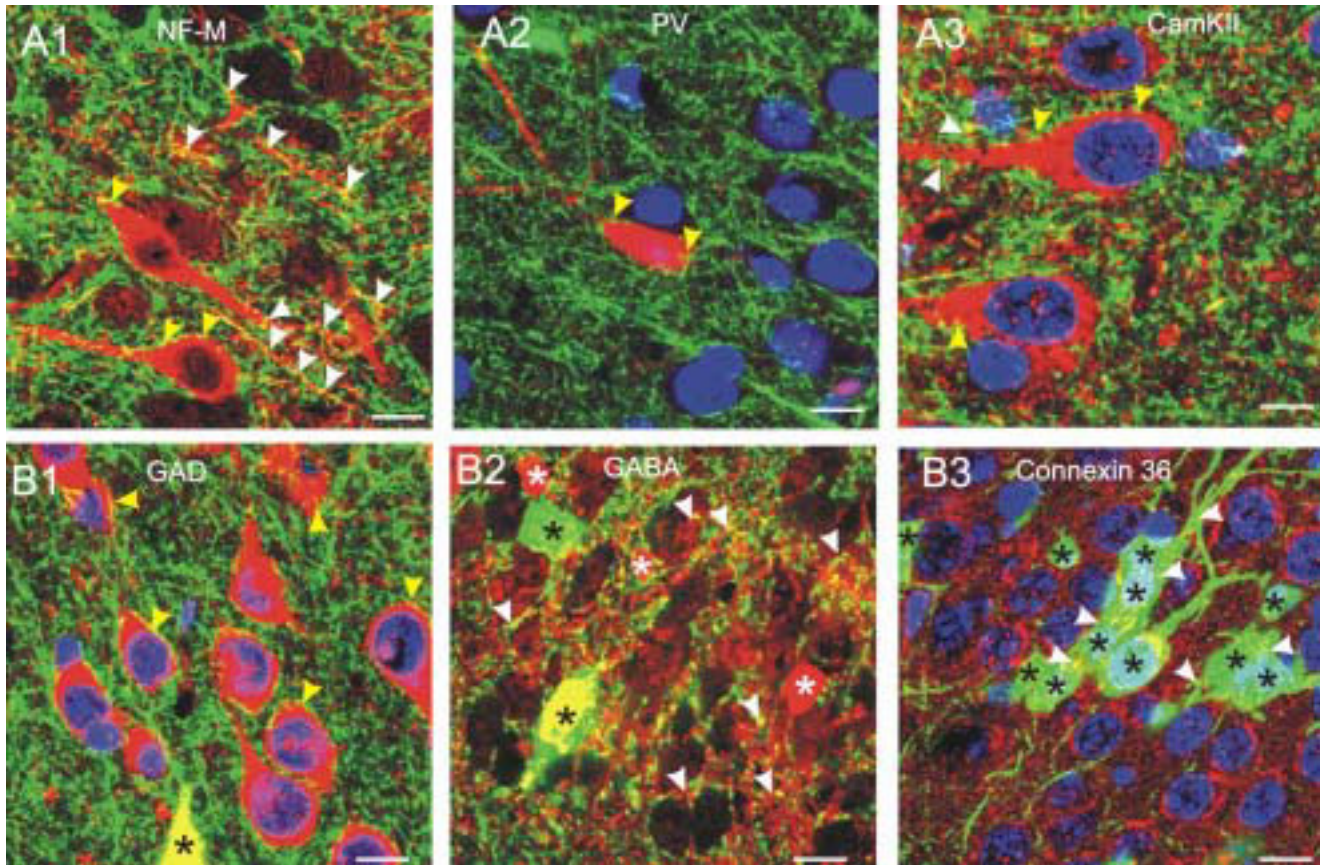
The Journal of Comparative Neurology. DOI 10.1002/cne

1012   C. ZHANG ET AL.

Fig. 10. **A:** High-magnification confocal image of three PPC sections with multiple labeling for GFP (green), and NF-M (A1, red), PV (A2, red), CamKII (A3, red), and nucleus (DAPI, blue). White arrowheads in A1–3: colocalization of presynaptic GFP varicosities with dendrites. Yellow arrowheads in A1–3: colocalization of presynaptic varicosities with cell bodies. **B:** Confocal image of three PPC sections with double labeling for GFP (green) and GAD (B1, red), GABA (B2, red), connexin36 (B3, red), and nucleus (DAPI, blue). Asterisks: GFP-positive cells that were also positive for GAD (B1), GABA (B2). White asterisks in B2: GABAergic cells. Yellow arrowheads in B1: colocalization of presynaptic GFP-positive varicosities with GAD-positive cell bodies. White arrowheads in B2: colocalization of GABA and GFP in presynaptic varicosities. White arrowheads in B3: colocalization of connexin36 with GFP-positive cell bodies and dendrites. Scale bars = 10 μm in A1,A2,B1,B2,B3; 5 μm in A3.

ronal subtype and the degree of similarity of the inhibitory networks to those of other sensory cortices was uncertain. To address these questions we took the advantage of the GAD65-EGFP mouse, in which abundant GFP-expressing GABAergic neurons were found in Layer II of the PPC. To our surprise, the GAD65-GFP-positive neurons were highly homogenous in electrophysiological and morphological properties.

Our first significant finding was that GABAergic neurons in the PPC showed a distinct subtype-dependent laminar composition. A novel subtype of GABAergic interneurons labeled by GAD65-EGFP was found in the Lamina II of PPC (Figs. 2, 3). These neurons outnumbered any other interneurons we have studied, including those expressing parvalbumin, calbindin, and calretinin (Fig. 9B1,B2). In the piriform cortex of the opossum, Haberly et al. (1983) noted an anterior–posterior difference in the absolute number of GABA labeled cells in Layer II, in that there were many more labeled cells in the posterior piriform cortex (15% in anterior vs. 30% in posterior piriform cortex). In that study, the highest number of labeled cells was in Layer III. A high concentration of labeled cells was also found in the subjacent endopiriform nucleus (EN). Presumably as a result of the dominance of non-GABAergic pyramidal cells in Layer II, the proportion of GABAergic cells was much lower in this layer than in

TABLE 1. Intrinsic Properties of GAD65-GFP Neurons in PPC

Neuronal types	Rem mV	R_{input} M°	τ ms	$ISF_{threshold}$ Hz	ISF_{max} Hz	Half width ms	Amplitude mV
GAD65-GFP	−64 ± 2	165 ± 25	16 ± 1	9 ± 1	65 ± 4	1.3 ± 0.3	87 ± 5

Rem: resting membrane potential; R_{input}: input resistance near rest; τ: membrane constant; $ISF_{threshold}$: near threshold interspike instant frequency; half width: action potential half-width; amplitude: amplitude of action potential; measurement was made from 8 GAD65-GFP cells.
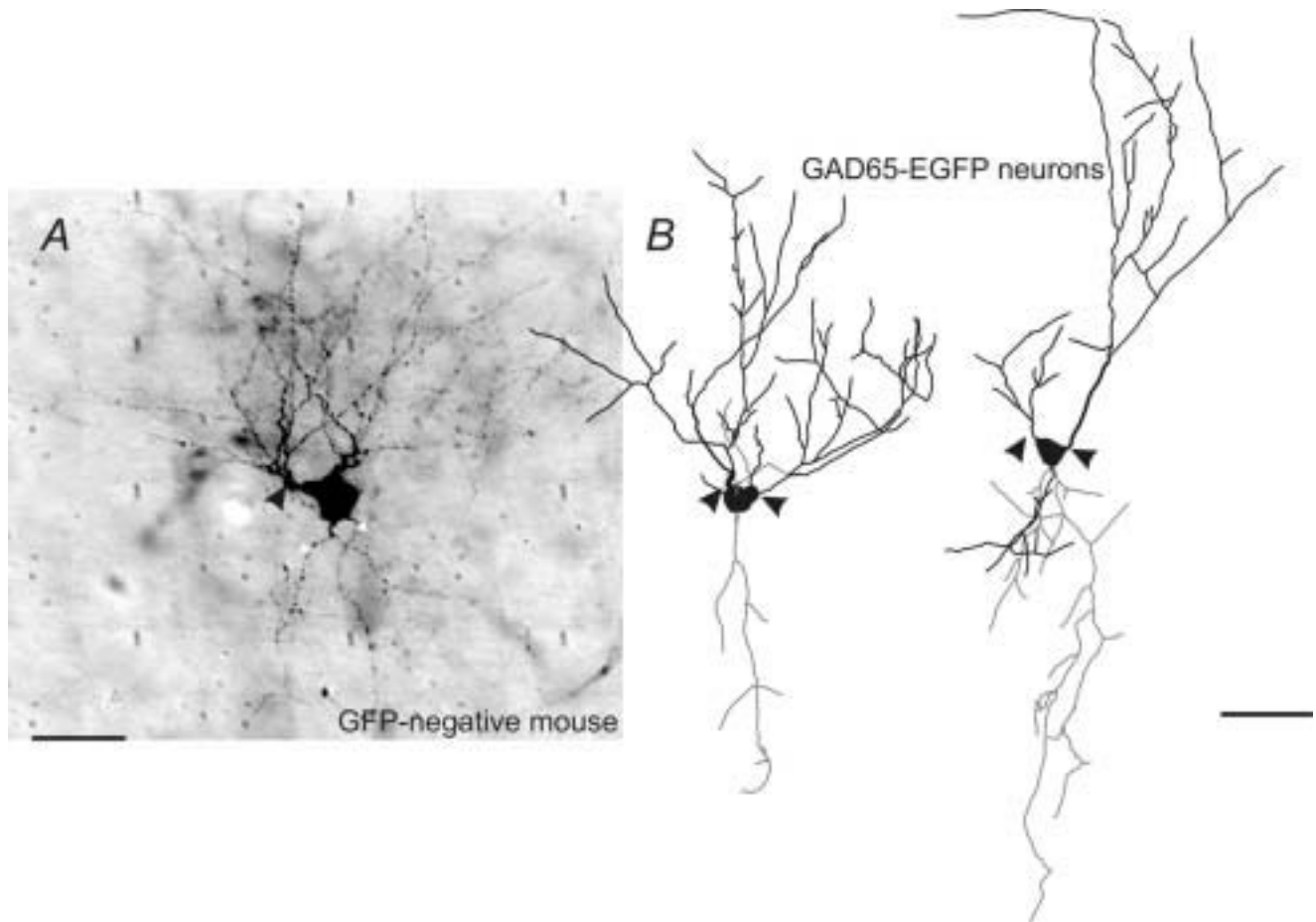
Fig. 11. **A:** Photomicrograph of intracellularly labeled regular-spiking nonpyramidal (RSNP) interneurons in the PPC of a GFP-negative mouse. Note that ascending dendrites were derived from two main thick dendritic branches (black arrowheads) near the cell body, while additional branching may occur more distally. The diameter of the upward dendrites usually gradually tapered toward the end. The branches of the ascending dendrites were oriented in a cluster toward the pia surface (not shown). These dendrites reached the outer portion of Layer I (pia surface). Dendritic spines were absent in this cell. The beaded appearance of the dendrites is common in cells stimulated electrophysiologically. The two main descending axons (white arrowheads) are derived from the lower portion of the cell body. The branches of the descending axons were oriented in a cluster toward the opposite direction of the dendritic tree and pia surface. **B:** Camera lucida drawings of two GAD65-EGFP neurons reconstructed from GAD65-EGFP cells. Black indicates dendrites and gray indicates axons. Note that the dendritic and axonal branching patterns of these two cells are similar to the cell in A. Black arrowheads: ascending dendrites were derived from two main thick dendritic branches. Scale bars = 50 μm.

Layers I and III (Haberly, 1983). In an earlier study in the rat brain, Mugnaini et al. (1984) reported that the piriform cortex contained only a few GABAergic cell bodies, between 5 and 15% of the total neuronal population. In a more recent study, Loscher et al. (1998) reported that GABAergic cell density was significantly higher in Layers II and III in posterior compared to more anterior sections and that the total number of GABAergic cells in Layer II was apparently higher than other layers throughout the posterior piriform cortex of the rat. Taken together, these results indicate a possibly species-dependent (opossum vs. mouse) laminar distribution of GABAergic cells in the PPC.

Our second significant finding was that the laminar distribution, somato-dendritic morphologies, and axonal arborizations of the GAD65-EGFP cells were all different from corresponding traits of PV cells and other interneurons expressing calcium-binding proteins (CB and CR). In the PPC of the domestic mouse, a dense PV axonal plexus formed a prominent band in Layer II that was clearly visible with low-power brightfield microscopy (Fig. 8). High-power images of the PV-positive axonal plexus revealed perisomatic boutons around unlabeled cells in Layer II, consistent with known features of basket cells. The PV cells were nonuniformly distributed in the PPC, with the majority of cells located in Layer III and the remainder located in superficial Layer II (Fig. 8). These features are similar to the PV cells in the rat piriform cortex (Ekstrand et al., 2001a,Ekstrand et al., 2001b) and multipolar basket cells in the neocortex (Kubota and Kawaguchi, 1994; Gabbott et al., 1997). However, in the mouse PPC the strong band of PV-immunopositive fibers in Layer II was formed by a much smaller population of basket cells (Figs. 7, 8). In the PPC of mouse, CR neurons were scattered in all layers (Fig. 9). These neurons shared similar dendritic morphological characters with CR neu-

rons in the neocortex (bipolar and double bouquet subtypes; cf. Jacobowitz and Winsky, 1991; Hof and Nimchinsky, 1992; Resibois and Rogers, 1992). The CB neurons were very sparse in PPC, mainly located near Layer II, and showed morphological characters of double bouquet cells (e.g., Fig. 9; cf. DeFelipe et al., 1989). Therefore, the interneurons expressing calcium-binding proteins in the PPC resembled their counterparts in the neocortex. In contrast, the GAD65-GFP neurons exhibited unique dendritic and axonal arborization patterns that were distinct from PV, CB, and CR cells in the piriform cortex and neocortex. Overall, less than 3% of the GAD65-EGFP neurons coexpressed calcium-binding proteins. This number was much lower than in neocortex, where ~40% of GABAergic interneurons expressed calcium-binding proteins (Hendry et al., 1989; DeFelipe et al., 1990). The lack of expression of calcium-binding proteins and unique laminar distribution of the GAD65-EGFP neurons indicate that these interneurons were distinct GABAergic types.

Another notable result was that the differences between GAD65-EGFP-expressing interneurons in the neocortex and the PPC were substantial. The most striking difference was that GAD65-GFP cells in the PPC coexpressed virtually none of the calcium-binding proteins that were abundantly expressed in neocortical GAD65-EGFP neurons. Of all cells counted in the neocortex, the proportion of GAD65-EGFP cells among CR-positive cells was 43% (n = 229), PV-positive cells 2% (Lopez-Bendito et al., 2004). In the PPC a negligible proportion of GAD65-EGFP neurons (<2%, Fig. 9A) coexpressed CR or CB and there was virtually no overlap between GFP cells and PV cells. In all layers of the neocortex, only 51% of the GABA-immunopositive cells were GAD65-EGFP-positive (Lopez-Bendito et al., 2004). Moreover, GAD65-EGFP cells in the PPC had unique laminar localization and represented the majority of the GABAergic neurons (~70%). The GAD65-EGFP neurons also had different dendritic and axonal morphology than their counterparts in the neocortex. Our results also showed that interneurons with similar laminar distribution and electrophysiological properties were found in wildtype and GFP-negative mice (Fig. 11). These data suggest that the unique properties of GAD65-EGFP neurons in the PPC were unlikely to have been induced by the exogenous expression of GFP in the GAD65-GFP mouse.

Of particular importance, our findings indicated a functional role for GAD65-GFP cells in olfactory-induced network oscillations and direct olfactory mediated feedforward inhibitory and disinhibitory processing. Both gamma (30–100 Hz) and theta (3–12 Hz) frequency oscillations have been found in the olfactory bulb (Eeckman and Freeman, 1990; Kay and Freeman, 1998) as well as the piriform cortex (Kay 1996). A necessary step toward understanding the mechanism underlying these oscillations is to have a thorough understanding of interneuronal subtypes within the olfactory-piriform cortical networks. Recent studies have established major neuronal subtypes (of glutamatergic and GABAergic types) within the piriform circuits. However, quantitative analysis of morphological properties of diverse groups of interneurons has been lacking. In the neocortex and hippocampus, three major functional classes of interneurons are recognized: 1) interneurons controlling principal cell output, 2) interneurons controlling dendritic inputs, and 3) long-range interneurons coordinating interneuron assemblies.

The number of neurons in a division shows an inverse relationship with spatial coverage. This type of connectivity-based classification is supported by the distinct physiological patterns of neuron class members in the intact brain (Buzsaki et al., 2004). In the PPC, the GAD65-EGFP neurons appear to fulfill all the roles mentioned above: i) control of principal cell outputs, ii) control of dendritic outputs, and iii) long-range interneuron coordination. The neuroanatomical evidence supporting these conclusions is: a) GAD65-EGFP inhibitory synapses are found in the perisomatic and particularly dendritic sites of presumed pyramidal neurons (e.g., Fig. 10); b) the dendritic and axonal arborization pattern of the GAD65-EGFP neurons; c) the location of GAD65-EGFP synapses onto dendrites and cell bodies of PV neurons that allows for controlling dendritic outputs of principal neurons (Fig. 10A2); and d) GAD65-EGFP neurons with gap junction connections that promote long-range synchronous interneuronal coordination (Fig. 6). Both electrical and chemical synaptic signaling between interneurons is crucial for network activity. Electrical coupling can selectively regulate the coherence of high-frequency network oscillations, whereas the time course of the chemical GABA$_A$-receptor-mediated component can control both coherence and frequency of network oscillations (Buzsaki and Draguhn, 2004). Furthermore, both electrical coupling between interneurons and disynaptic feedforward inhibition will promote synchrony detection in interneuron networks (Jonas et al., 2004). The characteristics of GAD65 cells fit very well with a role of promoting synchronous network activities of PPC.

In addition, our results indicate that the GAD65-GFP neurons may also play a distinct role in regulating information flow within the PPC. The dendrites of GAD65-GFP cells bifurcated extensively at superficial Lamina IA among horizontal afferent fibers. However, the axonal targets of the GAD65-GFP cells were restricted predominantly to Lamina III. This unique dendritic location and axonal targeting pattern suggests that these interneurons also play a role in direct olfactory-mediated feedforward inhibitory processes, much like the roles of basket cells in the somatosensory cortex. In the somatosensory cortices, sensory stimuli trigger precisely time-locked feedforward inhibitory responses mediated predominantly by basket cells (Sun et al., 2006). In the PPC, the sensory-mediated feedforward inhibition is likely to be mediated by GAD65-GFP cells, but not PV-positive basket cells, because the dendrites of PV cells are predominantly restricted to Layer III, which is not innervated by sensory afferents. Further electrophysiological experiments will be required to confirm the physiological roles of a distinct class of interneurons of PPC.

ACKNOWLEDGMENTS

LITERATURE CITED

Agmon A, Connors BW. 1991. Thalamocortical responses of mouse somatosensory (barrel) cortex in vitro. Neuroscience 41:365–379.

Beierlein M, Gibson JR, Connors BW. 2003. Two dynamically distinct

inhibitory networks in layer 4 of the neocortex. J Neurophysiol 90: 2987–3000.

Benes FM, Berretta S. 2001. GABAergic interneurons: implications for understanding schizophrenia and bipolar disorder. Neuropsychopharmacology 25:1–27.

Benson DL, Isackson PJ, Hendry SH, Jones EG. 1991. Differential gene expression for glutamic acid decarboxylase and type II calcium-calmodulin-dependent protein kinase in basal ganglia, thalamus, and hypothalamus of the monkey. J Neurosci 11:1540–1564.

Benson DL, Isackson PJ, Gall CM, Jones EG. 1992. Contrasting patterns in the localization of glutamic acid decarboxylase and Ca2+/calmodulin protein kinase gene expression in the rat central nervous system. Neuroscience 46:825–849.

Buzsaki G, Draguhn A. 2004. Neuronal oscillations in cortical networks. Science 304:1926–1929.

Buzsaki G, Geisler C, Henze DA, Wang XJ. 2004. Interneuron diversity series: circuit complexity and axon wiring economy of cortical interneurons. Trends Neurosci 27:186–193.

Chagnac-Amitai Y, Connors BW. 1989. Horizontal spread of synchronized activity in neocortex and its control by GABA-mediated inhibition. J Neurophysiol 61:747–758.

DeFelipe J. 1997. Types of neurons, synaptic connections and chemical characteristics of cells immunoreactive for calbindin-D28K, parvalbumin and calretinin in the neocortex. J Chem Neuroanat 14:1–19.

DeFelipe J, Hendry SH, Jones EG. 1989. Synapses of double bouquet cells in monkey cerebral cortex visualized by calbindin immunoreactivity. Brain Res 503:49–54.

DeFelipe J, Hendry SH, Hashikawa T, Molinari M, Jones EG. 1990. A microcolumnar structure of monkey cerebral cortex revealed by immunocytochemical studies of double bouquet cell axons. Neuroscience 37:655–673.

Eeckman FH, Freeman WJ. 1990. Correlations between unit firing and EEG in the rat olfactory system. Brain Res 528:238–244.

Ekstrand JJ, Domroese ME, Feig SL, Illig KR, Haberly LB. 2001a. Immunocytochemical analysis of basket cells in rat piriform cortex. J Comp Neurol 434:308–328.

Ekstrand JJ, Domroese ME, Johnson DM, Feig SL, Knodel SM, Behan M, Haberly LB. 2001b. A new subdivision of anterior piriform cortex and associated deep nucleus with novel features of interest for olfaction and epilepsy. J Comp Neurol 434:289–307.

Freeman WJ. 1978. Spatial properties of an EEG event in the olfactory bulb and cortex. Electroencephalogr Clin Neurophysiol 44:586–605.

Gabbott PL, Dickie BG, Vaid RR, Headlam AJ, Bacon SJ. 1997. Local-circuit neurons in the medial prefrontal cortex (areas 25, 32 and 24b) in the rat: morphology and quantitative distribution. J Comp Neurol 377:465–499.

Haberly LB. 1983. Structure of the piriform cortex of the opossum. I. Description of neuron types with Golgi methods. J Comp Neurol 213: 163–187.

Haberly LB, Feig SL. 1983. Structure of the piriform cortex of the opossum. II. Fine structure of cell bodies and neuropil. J Comp Neurol 216:69–88.

Haberly LB, Price JL. 1977. The axonal projection patterns of the mitral and tufted cells of the olfactory bulb in the rat. Brain Res 129:152–157.

Haberly LB, Price JL. 1978. Association and commissural fiber systems of the olfactory cortex of the rat. J Comp Neurol 178:711–740.

Hayes TL, Lewis DA. 1992. Nonphosphorylated neurofilament protein and calbindin immunoreactivity in layer III pyramidal neurons of human neocortex. Cereb Cortex 2:56–67.

Hendry SH, Jones EG, Emson PC, Lawson DE, Heizmann CW, Streit P. 1989. Two classes of cortical GABA neurons defined by differential calcium binding protein immunoreactivities. Exp Brain Res 76:467–472.

Hof PR, Nimchinsky EA. 1992. Regional distribution of neurofilament and calcium-binding proteins in the cingulate cortex of the macaque monkey. Cereb Cortex 2:456–467.

Hornung JP, Riederer BM. 1999. Medium-sized neurofilament protein related to maturation of a subset of cortical neurons. J Comp Neurol 414:348–360.

Jacobowitz DM, Winsky L. 1991. Immunocytochemical localization of calretinin in the forebrain of the rat. J Comp Neurol 304:198–218.

Jonas P, Bischofberger J, Fricker D, Miles R. 2004. Interneuron diversity series: fast in, fast out—temporal and spatial signal processing in hippocampal interneurons. Trends Neurosci 27:30–40.

Kay LM, Freeman WJ. 1998. Bidirectional processing in the olfactory-limbic axis during olfactory behavior. Behav Neurosci 112:541–553.

Kay LM, Lancaster LR, Freeman WJ. 1996. Reafference and attractors in the olfactory system during odor recognition. Int J Neural Syst 7:489–495.

Kubota Y, Jones EG. 1993. Co-localization of two calcium binding proteins in GABA cells of rat piriform cortex. Brain Res 600:339–344.

Kubota Y, Kawaguchi Y. 1994. Three classes of GABAergic interneurons in neocortex and neostriatum. Jpn J Physiol 44(Suppl 2):S145–S148.

Liu XB, Jones EG. 2003. Fine structural localization of connexin-36 immunoreactivity in mouse cerebral cortex and thalamus. J Comp Neurol 466:457–467.

Lopez-Bendito G, Sturgess K, Erdelyi F, Szabo G, Molnar Z, Paulsen O. 2004. Preferential origin and layer destination of GAD65-GFP cortical interneurons. Cereb Cortex 14:1122–1133.

Loscher W, Lehmann H, Ebert U. 1998. Differences in the distribution of GABA- and GAD-immunoreactive neurons in the anterior and posterior piriform cortex of rats. Brain Res 800:21–31.

Luskin MB, Price JL. 1983. The laminar distribution of intracortical fibers originating in the olfactory cortex of the rat. J Comp Neurol 216:292–302.

Markram H, Toledo-Rodriguez M, Wang Y, Gupta A, Silberberg G, Wu C. 2004. Interneurons of the neocortical inhibitory system. Nat Rev Neurosci 5:793–807.

McBain CJ, Fisahn A. 2001. Interneurons unbound. Nat Rev Neurosci 2:11–23.

McDonald AJ, Muller JF, Mascagni F. 2002. GABAergic innervation of alpha type II calcium/calmodulin-dependent protein kinase immunoreactive pyramidal neurons in the rat basolateral amygdala. J Comp Neurol 446:199–218.

Mugnaini E, Wouterlood FG, Dahl AL, Oertel WH. 1984. Immunocytochemical identification of GABAergic neurons in the main olfactory bulb of the rat. Arch Ital Biol 122:83–113.

Mullen RJ, Buck CR, Smith AM. 1992. NeuN, a neuronal specific nuclear protein in vertebrates. Development 116:201–211.

Price JL. 1999. Prefrontal cortical networks related to visceral function and mood. Ann N Y Acad Sci 877:383–396.

Price JL. 2003. Comparative aspects of amygdala connectivity. Ann N Y Acad Sci 985:50–58.

Prince DA. 1999. Epileptogenic neurons and circuits. Adv Neurol 79:665–684.

Resibois A, Rogers JH. 1992. Calretinin in rat brain: an immunohistochemical study. Neuroscience 46:101–134.

Sohl G, Maxeiner S, Willecke K. 2005. Expression and functions of neuronal gap junctions. Nat Rev Neurosci 6:191–200.

Sun QQ, Prince DA, Huguenard JR. 2003a. Vasoactive intestinal polypeptide and pituitary adenylate cyclase-activating polypeptide activate hyperpolarization-activated cationic current and depolarize thalamocortical neurons in vitro. J Neurosci 23:2751–2758.

Sun QQ, Baraban SC, Prince DA, Huguenard JR. 2003b. Target-specific neuropeptide Y-ergic synaptic inhibition and its network consequences within the mammalian thalamus. J Neurosci 23:9639–9649.

Sun QQ, Huguenard JR, Prince DA. 2006. Barrel cortex microcircuits: thalamocortical feedforward inhibition in spiny stellate cells is mediated by a small number of fast-spiking interneurons. J Neurosci 26: 1219–1230.

Westenbroek RE, Westrum LE, Hendrickson AE, Wu JY. 1987. Immunocytochemical localization of cholecystokinin and glutamic acid decarboxylase during normal development in the prepyriform cortex of rats. Brain Res 431:191–206.

Whittington MA, Traub RD. 2003. Interneuron diversity series: inhibitory interneurons and network oscillations in vitro. Trends Neurosci 26: 676–682.

Zou Z, Horowitz LF, Montmayeur JP, Snapper S, Buck LB. 2001. Genetic tracing reveals a stereotyped sensory map in the olfactory cortex. Nature 414:173–179.

Zou DJ, Greer CA, Firestein S. 2002. Expression pattern of alpha CaMKII in the mouse main olfactory bulb. J Comp Neurol 443:226–236.